

# Minimal self-contained quantum refrigeration machine based on four quantum dots

Davide Venturelli<sup>1,2</sup>, Rosario Fazio<sup>1</sup>, and Vittorio Giovannetti<sup>1</sup>

<sup>1</sup>*NEST, Scuola Normale Superiore and Istituto Nanoscienze-CNR, Piazza dei Cavalieri 7, I-56127 Pisa, Italy,*

<sup>2</sup>*Quantum Artificial Intelligence Laboratory, NASA Ames Research Center, Moffett Field CA 94035-1000.*

(Dated: September 8, 2018)

We present a theoretical study of an electronic quantum refrigerator based on four quantum dots arranged in a square configuration, in contact with as many thermal reservoirs. We show that the system implements the minimal mechanism for acting as a self-contained quantum refrigerator, by demonstrating heat extraction from the coldest reservoir and the cooling of the nearby quantum-dot.

PACS numbers: 03.65.Yz, 03.67.-a, 73.63.Kv, 73.23.-b

The increasing interest in quantum thermal machines has its roots in the need to understand the relations between thermodynamics and quantum mechanics [1, 2]. The progress in this field may as well have important applications in the control of heat transport in nano-devices [3]. In a series of recent works [4–6] the fundamental limits to the dimensions of a quantum refrigerator have been found. It has been further demonstrated that these machines could still attain Carnot-efficiency [5] thus launching the call for the implementation of the smallest possible quantum refrigerator. Refs.[4–6] considered self-contained thermal machines defined as those that perform a cycle without the supply of external work, their action being grounded on the steady-state heat transfer from thermal reservoirs at different temperatures. The major difficulty in the realization [7, 8] of self-contained refrigerators (SCRs) is the engineering of the crucial three-body interaction enabling the coherent transition between a doubly excited state in contact with a hot (H) and cold (C) reservoir, and a singly-excited state coupled to an intermediate (or “room” - R) temperature bath. We get around this problem by proposing an experimentally feasible implementation of a minimal SCR with semiconducting quantum dots (QDs) operating in the Coulomb blockade regime. We are thus able to establish a connection between the general theory of quantum machines and the heat transport in nanoelectronics [3].

QDs contacted by leads were proposed as ideal systems for achieving high thermopower [9–11] or anomalous thermal effects [12]. Here we study a four-QD planar array (hereafter named a “quadridot” for simplicity) coupled to independent electron reservoirs as shown in Fig. 1; with proper (but realistic) tuning of the parameters, we will show that the quadridot acts as a SCR which pumps energy *from* the high temperature reservoir H and the low temperature reservoir C *to* the intermediate temperature reservoirs R<sub>1</sub>, R<sub>2</sub>. Furthermore we will analyze the conditions under which the quadridot is able to cool the dot QD<sub>2</sub> which is directly connected to the bath C, at an effective temperature that is lower than the one it would have had in the absence of the other reservoirs. This will lead us to introduce an operative definition of the local effective temperature depending on the measurement

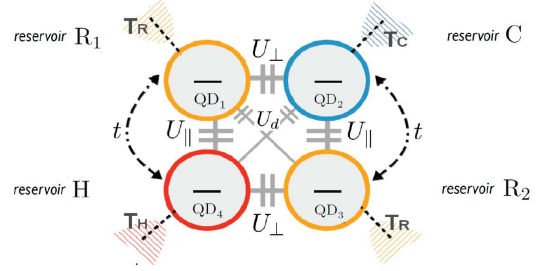


FIG. 1: [Color online] The quadridot. The four quantum dots QD<sub>1</sub>, QD<sub>2</sub>, QD<sub>3</sub>, and QD<sub>4</sub> are weakly coupled to the reservoirs R<sub>1</sub>, C, R<sub>2</sub>, and H, respectively, which are all grounded and maintained at temperatures  $T_H > (T_{R_1} = T_{R_2} = T_R) > T_C$ . Tunneling is allowed only between QD<sub>1</sub> and QD<sub>4</sub>, and between QD<sub>2</sub> and QD<sub>3</sub> ( $t$  being the gauging parameter).

setup, and to predict the existence of working regimes where, for instance, the refrigeration is not accompanied by the cooling of QD<sub>2</sub>. We start analyzing the system Hamiltonian, identifying the conditions that allows us to mimics the behavior of the SCR of Ref. [4].

In the absence of the coupling to the leads, the quadridot shown in Fig. 1 is described by the Hamiltonian

$$\mathcal{H}_{QD} = \sum_{i=1,\dots,4} \epsilon_i n_i + \sum_{i \neq j} \frac{U_{ij}}{2} n_i n_j - t(c_1^\dagger c_4 + c_2^\dagger c_3 + \text{h.c.}),$$

where for  $i = 1, \dots, 4$ ,  $c_i^\dagger$ ,  $c_i$ , and  $n_i = c_i^\dagger c_i$  represent respectively the creation, annihilation and number operators associated with the  $i$ -th QD. In this expression the quantities  $\epsilon_i$  gauge the single particle energy levels,  $t$  defines the tunneling coupling between the dots, and  $U_{ij}$  describes the finite-range contribution of the Coulomb repulsion. To reduce the maximum occupancy in each QD to one electron, we will assume the on-site repulsion terms  $U_{ii}$  to be the largest energy scale in the problem. Furthermore, in order to mimic the dynamics of [4] we will take  $U_{12} = U_{34} = U_\perp$  and  $U_{23} = U_{14} = U_\parallel$ , both much larger than the “diagonal” terms  $U_{24} = U_{13} = U_d$ , and tune the single-electron energy level of the upper-right dot (which will be coupled to the cool reservoir C) so that  $\epsilon_2 = \epsilon_1 + \epsilon_3 - \epsilon_4$ . These choices ensure that in the

absence of tunneling ( $t = 0$ ), the “diagonal” two-particle states  $|d\rangle = |1, 0, 1, 0\rangle$  and  $|\bar{d}\rangle = |0, 1, 0, 1\rangle$  shown in Fig. 2 are degenerate (the charge states are labeled according to the occupation of the four dots  $|n_1, n_2, n_3, n_4\rangle$ ). These are the only states of the two-electron sector which play an active role in the system evolution, mimicking the role of the vectors  $|01\rangle$ ,  $|10\rangle$  of [4]. Due to the presence of  $U_\perp$  or  $U_\parallel$  the other configurations are indeed much higher in energy to get permanently excited in the process. Still the states  $|u\rangle = |1, 1, 0, 0\rangle$  and  $|l\rangle = |0, 0, 1, 1\rangle$  play a fundamental role in the SCR as their presence generates (via a Schrieffer-Wolff transformation [13, 14] and the non-zero hoppings  $t$ ) an effective coupling term between  $|d\rangle$  and  $|\bar{d}\rangle$  of the form  $H_{eff} = g_{d\bar{d}}(|d\rangle\langle\bar{d}| + |\bar{d}\rangle\langle d|)$  with

$$g_{d\bar{d}} \simeq \frac{2t^2(U_d - U_\perp)}{(U_d - U_\perp)^2 - (\epsilon_4 - \epsilon_1)^2} \ll t. \quad (1)$$

In our model  $g_{d\bar{d}}$  is the analogous of the perturbative parameter  $g$  of [4]. Its role is to open a devoted channel which favors energy exchanges between the couple H-C and the couple R<sub>1</sub>-R<sub>2</sub> by allowing two electrons to pass from the first to the second through the mediation of the quadridot states  $|\bar{d}\rangle$  [which is in contact with H and C] and  $|d\rangle$  [which is connected to R<sub>1</sub> and R<sub>2</sub>]. For proper temperature imbalances this is sufficient to establish a positive heat flux *from C to QD<sub>2</sub>* even if  $T_C$  is the lowest of all bath temperatures. The mechanisms can be heuristically explained as follows: if  $T_H$  is sufficiently higher than the other bath temperatures, then the dot which has more chances of getting populated by its local reservoir is QD<sub>4</sub>. When this happens, the large values of  $U_\perp$ ,  $U_\parallel$  will prevent QD<sub>1</sub> and QD<sub>3</sub> from acquiring electrons too. On the contrary, while QD<sub>4</sub> is populated, QD<sub>2</sub> is allowed to accept an electron from its reservoir C [ $U_d$  being much smaller than  $U_\perp$ ,  $U_\parallel$ ] creating  $|\bar{d}\rangle$ . The coupling provided by  $H_{eff}$  will then rotate the latter to  $|d\rangle$  giving the two electrons [the one from H and the one from C] a chance of being absorbed by R<sub>1</sub>-R<sub>2</sub>. The opposite process (creation of  $|d\rangle$  by absorption of a couple of electrons from R<sub>1</sub>-R<sub>2</sub>, rotation to  $|\bar{d}\rangle$ , and final emission toward H-C) is statistically suppressed due to the (relatively) low probability that QD<sub>1</sub> or QD<sub>3</sub> will get an electron from their reservoir before QD<sub>4</sub> gets its own from H: the net result is a positive energy flux from H-C to R<sub>1</sub>-R<sub>2</sub>.

To verify this picture we explicitly solve the open dynamics of the quadridot and study its asymptotic behavior. Specifically, we model our four local baths H, C, R<sub>1</sub> and R<sub>2</sub> as independent electron reservoirs (leads) characterized by their own chemical potential  $\mu_i$  and their own temperature [both quantities entering in the Fermi-Dirac occupation functions  $f_i(\epsilon)$  associated with the reservoir]. For the sake of the simplest correspondence with the model of Ref. [4] in this study all  $\mu_i$  will be set to be identical and fixed to a value that will be used as reference for the single particle energies of the system [e.g. setting  $\epsilon_i = 0$  in the Hamiltonian corre-

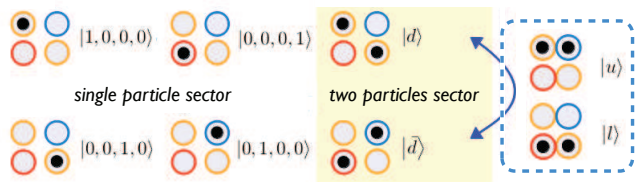


FIG. 2: [Color online] Pictorial view of the low-energy electronic charged states (a black circle indicates occupation by an electron). Due to the hoppings terms  $t$  and  $g_{d\bar{d}}$  the eigenstates of the low-energy Hamiltonian are bonding-antibonding states  $|d\rangle \pm |\bar{d}\rangle$  and the four bonding-antibonding delocalized single particles states (the completely empty state is not shown). For  $t = 0$  the two electron states  $|d\rangle$  and  $|\bar{d}\rangle$  are resonant, while  $|u\rangle$  and  $|l\rangle$  are the high-energy virtual states responsible for the effective interaction  $g_{d\bar{d}}$  coupling  $|d\rangle$ ,  $|\bar{d}\rangle$ .

sponds to have the  $i$ -th quadridot level at resonance with the Fermi energy of the reservoirs]. Furthermore as detailed in the caption of Fig. 1 the temperatures will be chosen to satisfy the relation  $T_C < T_{R_1} = T_{R_2} < T_H$  [15]. Within these assumptions, the only required external action is exerted in maintaining the local equilibrium temperatures and chemical potential, in accordance to the standard definition of self-containment. The quadridot-bath couplings (parametrized by the amplitudes  $\Gamma_i^{(k)}$ ) are hence expressed as tunneling terms of the form

$$H_T = \sum_{i=1,\dots,4} \sum_k \Gamma_i^{(k)} c_i^\dagger a_{i,k} + \text{h.c.} \quad (2)$$

with  $a_{i,k}$  being an annihilation operator which destroy an electron of momentum  $k$  in the lead  $i$ . In the Born-Markov-Secular limit [17, 18] these extra terms, give rise to a Lindblad equation for the reduced density matrix  $\rho$  of the quadridot. The presence of  $t$  plus the rotation into the low-energy sector eliminates degeneracies among all possible energy transitions between the eigenstates of the quadridot. The evolution of  $\rho$  is then determined by

$$\dot{\rho} = \sum_i \mathcal{D}_i[\rho], \quad (3)$$

where for each reservoir  $\mathcal{D}_i$  represents associated Lindblad dissipator. This equation can be solved in the steady-state regime ( $\dot{\rho} = 0$ ) yielding the asymptotic configuration  $\rho^\infty$ , from which the heat currents  $\langle \mathbf{J}_{Q,i} \rangle$  flowing through the  $i$ -th reservoir are then computed as [17],

$$\langle \mathbf{J}_{Q,i} \rangle = \text{Tr} \left[ \mathcal{H}_{QD} \mathcal{D}_i[\rho^\infty] \right]. \quad (4)$$

If our implementation of the SCR is correct, we should see a direct heat flow *from* the hot H and cold C reservoirs *to* the reservoirs R<sub>1</sub> and R<sub>2</sub>, while the dot QD<sub>2</sub> should reach an occupation probability corresponding to an effective temperature which is lower than the one dictated by its local reservoir C (See Fig. 3-b). We have

verified this by setting the system parameters to be consistent with those presented in [4] – making sure however that for such choice no additional degeneracies are introduced into the system due to the larger dimension of our physical model. While the performances of the device do not change qualitatively when varying the parameters according to above prescriptions, in the following we focus on a specific scenario where we fixed  $\epsilon_1 = 2.1$ ,  $\epsilon_3 = 2.9$ ,  $\epsilon_4 = 4.0$ , and  $U_\perp = 12.0$  [ $U_\parallel$  instead is taken to be infinitely large for simplicity as its effect could be absorbed in the energy level renormalization after the Schrieffer-Wolff transformation]. The value of  $g_{d\bar{d}}$  is finally taken to be  $-0.001$  determining  $t$  ( $\lesssim 0.1$ ) through Eq. (1), while the couplings terms  $\Gamma_i^{(k)}$  which link the quadridot to the reservoirs via Eq. (2) are chosen to provide effective dissipation rates of order  $\sim 0.0001$  [19]. Solving numerically the steady state equation (3) we observe that for each  $T_C < T_R$ , there exists a minimal threshold value for  $T_H$  above which the SCR indeed extracts heat from the cold reservoir C. This is shown in Fig. 3-a for  $T_R=2$  and different values of  $U_d$ , the quadridot works as a SCR in the blue region. Consistently with the second principle of thermodynamics the threshold value of  $T_H$  (black curve in the plot) is always greater than  $T_R = 2$  (for  $T_H$  below  $T_R$  the machine cannot produce work from H to pump heat from C), and that the region above this threshold gets larger as  $U_d$  gets smaller. The existence of a threshold for  $T_H$  implies also that, for given  $T_H > T_R$ , there is a minimal temperature  $T_C^*$  for the cold reservoir under which the SCR cannot work. Interestingly for  $T_H/T_R \rightarrow \infty$  the value of  $T_C^*$  appears to asymptotically converge toward a finite non-zero temperature which depends upon the engine microscopic parameters and which can be interpreted as *the emergent absolute zero* of the model. An approximate analytical expression for  $T_C^*$  can be derived exploiting the recent general theory of genuine, maximally-efficient self-contained quantum thermal machines [6]. This is done by interpreting the quadridot as a composite system, consisting of an “effective” virtual qubit formed by the states  $|0, 0, 0, 1\rangle$  and  $|d\rangle$  which (through  $g_{d\bar{d}}$ ) mediates the interaction between QD<sub>2</sub> and the reservoirs H, R<sub>1</sub> and R<sub>2</sub>. The average occupations of the virtual qubit levels (determined by the coupling with the reservoirs H, R<sub>1</sub> and R<sub>2</sub>) defines the effective (average) temperature of H, R<sub>1</sub> and R<sub>2</sub> which is perceived by QD<sub>2</sub>: such temperature competes with  $T_C$  in cooling down the dot and can be identified with the value of  $T_C^*$  of our model. Observing that the energy levels of  $|0, 0, 0, 1\rangle$  and  $|d\rangle$  are  $\epsilon_4$ ,  $\epsilon_1 + \epsilon_3 + U_d$  respectively, from [6] we get

$$T_C^* \simeq T_R T_H \frac{\epsilon_1 + \epsilon_3 + U_d - \epsilon_4}{T_H(\epsilon_1 + \epsilon_3 + U_d) - T_R \epsilon_4}, \quad (5)$$

which fits pretty well our numerical results (See Fig. 3-a) and which for  $T_H \rightarrow \infty$  yields  $T_R(1 - \epsilon_4/[\epsilon_1 + \epsilon_3 + U_d])$  as emergent absolute zero of the model.

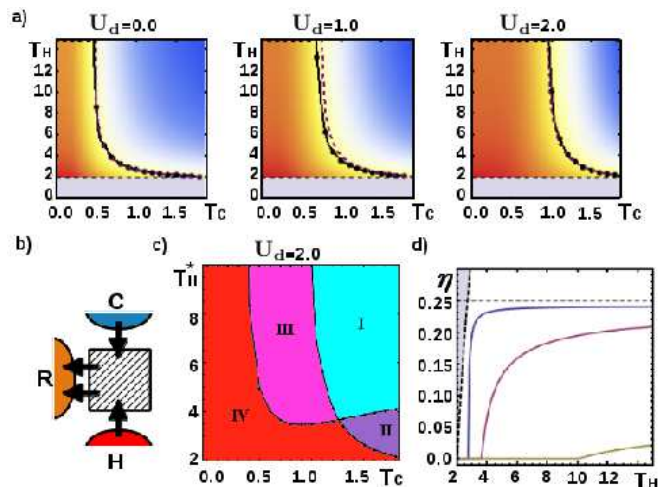


FIG. 3: [Color online] a) Panels refer to  $U_d = 0$  (left),  $U_d = 1$  (center),  $U_d = 2$  (right). When  $T_H$  approaches the black curve, i.e. at values very close to the analytical value of Eq. (5) (dashed line), a change of sign in the heat flow occurs. For  $T_H$  above the threshold (blue region) the machine works as pictured in b), extracting heat from the C,H-reservoirs and pumping it into R. In the opposite regime (red region) heat cannot be extracted from C. Black dashed line above the grey region indicates  $T_H = T_R = 2$ . Blue/Red background color intensity is proportional to the actual heat pumped to/extracted from C. c) Comparison between heat extraction and single particle occupation for  $U_d = 2$ . In regions I/II the SCR is working (heat is extracted from C) while in regions III/IV the C bath receives heat. In regions I/III we have an effective decrease of the occupation number of QD<sub>2</sub> (i.e.  $\langle n_2 \rangle < \langle n_2^0 \rangle$ ). d) Efficiency of the SCR compared to the Carnot efficiency (dashed black line) for  $T_C = 1.0$ . The curves represent  $U_d = 0$  (blue),  $U_d = 1$  (magenta) and  $U_d = 2$  (brown). The dashed horizontal line indicates maximum limit of efficiency for the quadridot computed (for  $U_d = 0$ ) as in [4].

Following [5], we evaluate the ratio  $\eta = \langle \mathbf{J}_{Q,2} \rangle / \langle \mathbf{J}_{Q,4} \rangle$  between the heat current through the cold and hot reservoirs comparing it with the upper bound  $(1 - \frac{T_R}{T_H}) / (\frac{T_R}{T_C} - 1)$  posed by the Carnot limit, and with the theoretical value  $\eta_{th} = (\epsilon_1 + \epsilon_3 - \epsilon_4) / \epsilon_4$  of [4] applied to the quadridot for  $U_d = 0$  [20]. The dependence of  $\eta$  upon  $T_H$  is plotted in Fig. 3-d for different values of  $U_d$ . We noticed that in the case  $U_d = 0$  the efficiency of the quadridot converges indeed towards the theoretical value  $\eta_{th}$  of [4] at least for large enough  $T_H$ .

*Measurements and effective local temperatures:*— An important question is whether this refrigeration effect is accompanied with a cooling of QD<sub>2</sub>, namely whether its effective local temperature  $T_C^{(eff)}$  decreases as  $T_H$  increases, for sufficiently high  $T_H$ , in analogy with the qubit-cooling described in Ref. [4]. While for such idealized qubit model the definition of the local temperature is relatively straightforward, in nanoscale systems out of equilibrium, local temperatures must be *operationally* defined [21]. The most common way to proceed

is to introduce a probe reservoir P (a “thermometer”) which is weakly coupled to that part of the system we are interested in (the dot QD<sub>2</sub> in our case) and identify the effective temperature of the latter with the value of the temperature  $T_P$  of the probe which nullifies the heat flow through P. This procedure yields a natural way of measuring the effect we are describing and can be implemented easily in our model by adding an extra term in (2) that connects the new reservoir P to QD<sub>2</sub> with a tunnel amplitude  $\Gamma_P$  which is much smaller than those associated with the other reservoirs of the system (in the calculation we set the ratio between  $\Gamma_P$  and  $\Gamma_i$  of the other reservoirs to be of the order  $10^{-3}$ : this make sure that the presence of P does not perturb the system). The obtained values of  $T_C^{(eff)}$  are presented in Fig. 3-a where it is shown that, according to this definition of the local temperature, the conditions for cooling of QD<sub>2</sub> (i.e.  $T_C^{(eff)} < T_C$ ) are the same for the SCR to work (implying incidentally that in this case  $T_C^{(eff)}$  is always greater than the emergent zero-temperature of the system  $\bar{T}_C$ ).

The quantity  $T_C^{(eff)}$  introduced above has a clear operational meaning and according to the literature it is a good candidate to define the effective temperature of QD<sub>2</sub>. Still it is important to acknowledge that in experiments the cooling of QD<sub>2</sub> can also be detected by using the non-invasive techniques of e.g. Ref. [22] to look at the decrease of the mean asymptotic occupation number of QD<sub>2</sub>,  $\langle n_2 \rangle = \langle 0, 1, 0, 0 | \rho^\infty | 0, 1, 0, 0 \rangle + \langle d | \rho^\infty | d \rangle$ , with respect to the same quantity computed when the SCR is “turned off” (e.g.  $\langle n_2^0 \rangle = \langle 0, 1, 0, 0 | \rho_0^\infty | 0, 1, 0, 0 \rangle + \langle d | \rho_0^\infty | d \rangle$  where now  $\rho_0^\infty$  is the asymptotic stationary state of the system reached when all the reservoirs but C are disconnected, i.e.  $\Gamma_{i \neq C} = 0$ ). We notice however that the cooling condition hereby defined does not coincide with the same pictured in Fig. 3-a. We indeed exemplify in Fig. 3-c for  $U_d=3$  that according to this new definition different operating regimes are possible for the SCR. The QD<sub>2</sub> might be either colder ( $n_2 < n_2^0$  in zone I) or hotter ( $n_2 > n_2^0$ , in region II) when the device extract heat from the C reservoir. Conversely, we might achieve a colder QD<sub>2</sub> also when the quadridot pumps heat into the colder bath (III). In region IV none of the refrigeration effects are active. Similar regimes emerge with other activation prescriptions, such as defining  $\langle n_2^0 \rangle$  as the occupation for  $T_H = T_R = T_C$  while maintaining all tunnel couplings as constant.

*Conclusions:*— We conclude with experimental considerations. Quadridots in GaAs/AlGaAs heterostructures have been implemented for Cellular-Automata computation [23] and for single-electron manipulation [24]. Strongly capacitively-coupled QDs with interdot capacitance energy ( $U_\perp$  and  $U_\parallel$ ) up to 1/3 of the intra-dot charging energy (taken to be infinite in our model) can be fabricated with current lithographic techniques [25]. The diagonal inter-dot term  $U_d$  is expected to be at most

$U_\parallel/\sqrt{2} \simeq U_\perp/\sqrt{2}$  from geometrical considerations, but practically it is expected to be much smaller [24]. The local charging energy can be as big as 1 meV, and usually represents about 20% of the confinement energy [26], which is the typical tunable values of the single-particles levels  $\epsilon_i$ . Charging effects are expected to be further enhanced by the presence of a significant magnetic field, due to the emergence of the incompressible antidot regime in the dots [27], possibly allowing the working conditions to be achieved even more easily. In this high-field regime, the spin/orbital-Kondo effect [28, 29] is suppressed [30], as the transport becomes spin-polarized, so our effective description is expected to be valid. A final ingredient for the quadridot to act as a SCR is quantum coherence. In QDs it is known that the main source of decoherence comes from  $1/f$  noise arising from background charge fluctuations [31] (however coherent manipulation of QDs have been reported in several experiments, e.g. see Ref. [32]). Accordingly Eq. (3) acquires an extra contribution whose effect (see Supplemental Material [33]) is to modify the steady state populations. In our setup as long as the new rates are of the same order of the ones due to the coupling to the leads the quadridot will still work as a SCR (note, indeed, that the bounds to the blue region in Fig. 3 a) do not depend on these rates). Possibly the only serious challenge is posed by the need that the induced broadening should not be too large with respect to  $t$ . For the sake of simplicity we adopted small values of this parameter, however it is very much possible that higher values will help the efficiency of the SCR by speeding up the  $|d\rangle$ ,  $|\bar{d}\rangle$  rotations. We finally observe that the maximum thermal energies involved should not exceed the large charging energies (i.e.  $\lesssim 10K$ ).

We acknowledge useful discussions with C.W.J. Beenakker, M. Carroll, F. Giazotto, F. Mazza, and J. Pekola and support from MIUR through the FIRB-IDEAS project RBID08B3FM, by EU through the Project IP-SOLID, and by Sandia National Laboratories.

- 
- [1] G. Gemma, M. Michel and G. Mahler, *Quantum Thermodynamics*, Springer (Berlin, 2004).
  - [2] K. Maruyama, F. Nori, and V. Vedral, Rev. Mod. Phys. **81**, 1 (2009); M. Esposito, H. Harbola, and S. Mukamel, Rev. Mod. Phys. **81**, 1665 (2009).
  - [3] F. Giazotto, T. T. Heikkilä, A. Luukanen, A. M. Savin, and J. P. Pekola, Rev. Mod. Phys. **78**, 217 (2006).
  - [4] N. Linden, S. Popescu, and P. Skrzypczyk, Phys. Rev. Lett. **105**, 130401 (2010).
  - [5] P. Skrzypczyk, N. Brunner, N. Linden, and S. Popescu, J. Phys. A Math. Theor. **44**, 492002 (2011).
  - [6] N. Brunner, N. Linden, S. Popescu, and P. Skrzypczyk, Phys. Rev. E **85**, 051117 (2012).
  - [7] Y. Chen, and S. Li, Europhys. Lett. **97**, 40003 (2012).
  - [8] A. Levy and R. Kosloff, Phys. Rev. Lett. **108**, 070604 (2012).

- [9] C. W. J. Beenakker and A. A. M. Staring, Phys. Rev. B **46**, 9667 (1992).
- [10] D. Bose and R. Fazio, Europhys. Lett. **56**, 576 (2001).
- [11] P. Trocha and J. Barnaś, Phys. Rev. B **85**, 085408 (2012).
- [12] R. Sánchez, R. López, D. Sánchez, and M. Büttiker, Phys. Rev. Lett. **104**, 076801 (2010); R. Sánchez and M. Büttiker, Phys. Rev. B **83**, 085428 (2011).
- [13] J. R. Schrieffer and P. A. Wolff, Phys. Rev. **149**, 491 (1966).
- [14] S. Bravyi, D. P. DiVincenzo, and D. Loss, Annals of Physics **326**, 2793 (2011).
- [15] Having set  $T_{R_1} = T_{R_2} = T_R$ ,  $R_1$  and  $R_2$  can be considered a single incoherent reservoir: this hypothesis is not strictly necessary but it helps in simplifying the analysis.
- [16] As discussed in Ref. [12], the energy dependence of the local density of states and the tunneling amplitudes in contacted QDs alone can be the origin of interesting thermal effects. While this additional degree-of-freedom may perhaps be used to shape the working regions of the SCR, we consider for simplicity these energy dependence to be negligibly varying over the ranges of our energy splitting.
- [17] H.P. Breuer and F. Petruccione, *The Theory of Open Quantum Systems* (Oxford University Press, Oxford 2002).
- [18] G. Schaller, Course Lecture Notes “Non-Equilibrium Master Equations” (2012) and G. Schaller, G. Kiesslich, and T. Brandes, Phys. Rev. B **80**, 245107 (2009)
- [19] Indicatively, to be experimentally reasonable, the energy units should be considered as multiples of 100  $\mu\text{eV}$ .
- [20] Not null values of the parameter  $U_d$  introduce Coulomb interactions among degenerate resonant states which tend to spoil the correspondence with the three qubit system of Ref. [4]. In our case however it is not realistic to assume  $U_d = 0$  so we keep it small but not null. It turns out that the performances of the system are not significantly affected by this choice (e.g. see Fig. 3).
- [21] H. L. Engquist and P. W. Anderson, Phys. Rev. B **24**, 1151 (1981).
- [22] R. Schleser, *et al.*, Appl. Phys. Lett. **85**, 2005 (2004); L. DiCarlo, *et al.*, Phys. Rev. Lett. **92**, 226801 (2004); C. B. Simmons, *et al.*, Nano Lett. **9**, 3234 (2009); S. Gasparinetti, *et al.*, Appl. Phys. Lett. **100**, 253502 (2012).
- [23] F. Perez-Martinez, *et al.*, Appl. Phys. Lett. **91**, 032102 (2007).
- [24] R. Thalineau, S. Hermelin, A. D. Wieck, C. Bäuerle, L. Saminadayar, and T. Meunier, Appl. Phys. Lett. **101**, 103102 (2012).
- [25] I. H. Chan, R. M. Westervelt, K. D. Maranowski, and A. C. Gossard, Appl. Phys. Lett. **80**, 1818 (2002).
- [26] A. Hübner, J. Weis, W. Dietsche, and K. v. Klitzing, Appl. Phys. Lett. **91**, 102101 (2007).
- [27] H. van Houten, C. W. J. Beenakker, and A. A. M. Staring, *Single Charge Tunneling*, edited by H. Grabert and M. H. Devoret, NATO ASI Series B, Vol. 294, (Plenum Press, New York, 1992).
- [28] L. Borda, Gergely Zaránd, W. Hofstetter, B. I. Halperin, and J. von Delft, Phys. Rev. Lett. **90**, 026602 (2003).
- [29] D. E. Liu, S. Chandrasekharan, and H. U. Baranger, Phys. Rev. Lett. **105**, 256801 (2010).
- [30] Y. Meir, N. S. Wingreen, and P. A. Lee, Phys. Rev. Lett. **70**, 2601 (1993).
- [31] K. D. Petersson, J. R. Petta, H. Lu, and A. C. Gossard, Phys. Rev. Lett. **105**, 246804 (2010).
- [32] T. Hayashi, T. Fujisawa, H. D. Cheong, Y. H. Jeong, and Y. Hirayama Phys. Rev. Lett. **91**, 226804 (2003); L. DiCarlo, H. J. Lynch, A. C. Johnson, L. I. Childress, K. Crockett, C. M. Marcus, M. P. Hanson, and A. C. Gossard Phys. Rev. Lett. **92**, 226801 (2004).
- [33] Supplemental Material is available online at: <http://prl.aps.org/supplemental/PRL/v110/i25/e256801>